How to cite: *Angew. Chem. Int. Ed.* **2023**, e202311734
doi.org/10.1002/anie.202311734

Catalysis

Single Chain Nanoparticles in Catalysis

Kai Mundsinger[+], *Aidan Izuagbe*[+], *Bryan T. Tuten*,* *Peter W. Roesky*,* *and Christopher Barner-Kowollik**

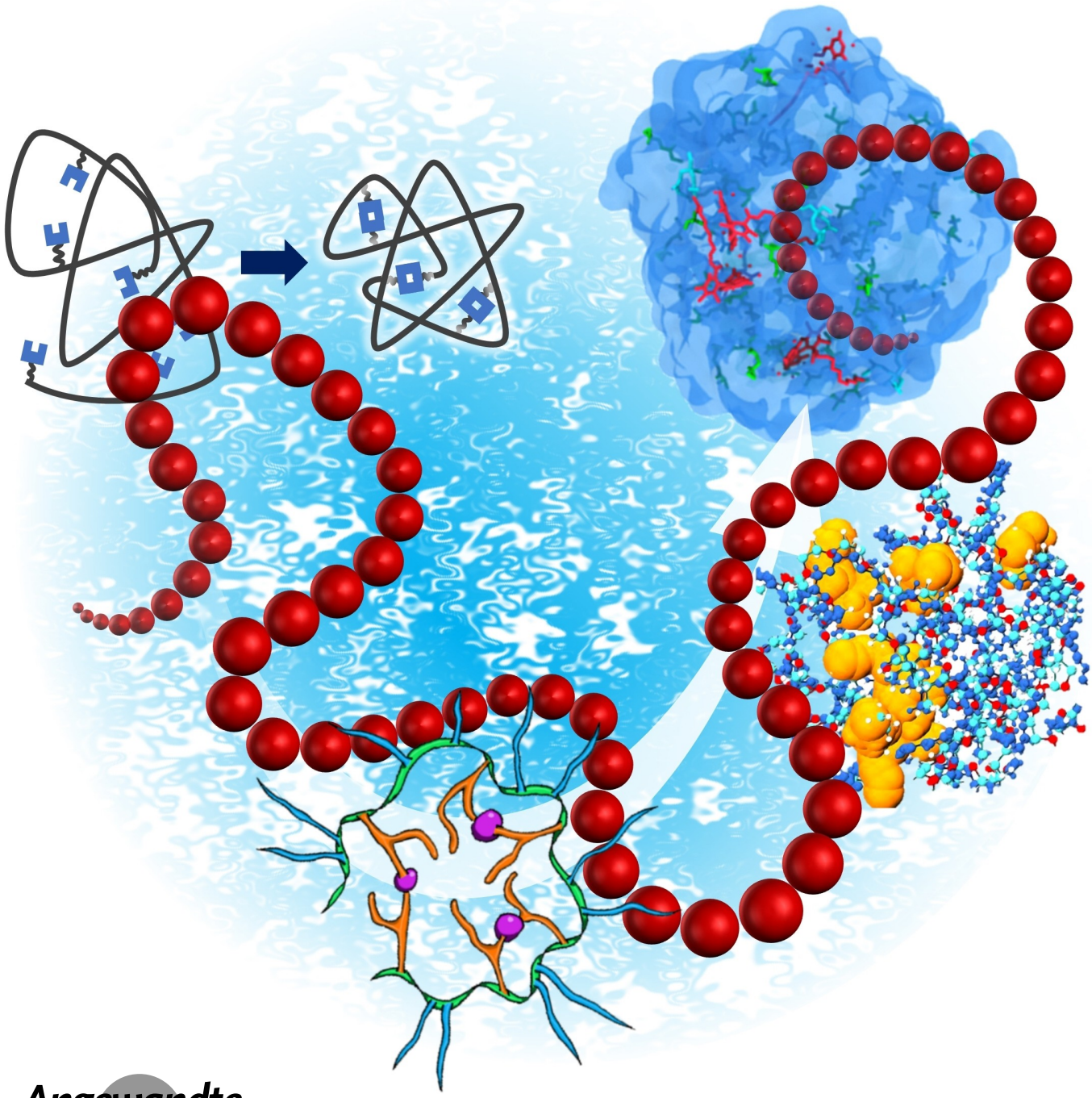

Abstract: Over the last six decades folded polymer chains—so-called Single Chain Nanoparticles (SCNPs)—have evolved from the mere concept of intramolecularly crosslinked polymer chains to tailored nanoreactors, underpinned by a plethora of techniques and chemistries to tailor and analyze their morphology and function. These monomolecular polymer entities hold critical promise in a wide range of applications. Herein, we highlight the exciting progress that has been made in the field of catalytically active SCNPs in recent years.

1. Introduction

Precision control over macromolecular architecture has been the aim of polymer chemists ever since the early inception of the field by Hermann Staudinger's macromolecular hypothesis in the 1920s.[1] In the natural world, proteins serve as functional macromolecules playing key roles from cell signalling and immune responses[2] to gene expression and regulation,[3] fulfilling functions in chemically complex environments with high efficiency and precision. Proteins' catalytic abilities are owed to their geometric precision, afforded by a sequence defined primary structure of amino acid building blocks. Nowhere in biochemistry is this precision folding more evident than in the role of enzymes, which are responsible for catalysing nearly all chemical reactions that occur within living organisms.[4] Precise folding of enzymes leads to the formation of catalytic pockets which allow for specific binding of substrates, where the complex macromolecular scaffold accommodates only specific substrates, while helping to stabilise the transition states of the reaction.[5] The synergy between macromolecular architecture and catalytic site constitutes the blue print for chemists attempting to develop advanced 'bio-inspired' polymeric catalysts. Single chain nanoparticles (SCNP) comprised of single polymers folded intramolecularly into discrete nanoparticles combined with catalytic functionality have been implemented as one of many 'bio-inspired' polymeric catalysts. The earliest SCNPs were merely structural, consisting of intramolecular crosslinks employed to induce chain collapse into a nanoparticle.[6–8] Initial interest was focused on changes in intrinsic viscosity and radius of gyration upon chain collapse.[7,9–12] The field was dormant for nearly two decades until the utilisation of new methodologies for polymer synthesis[13–15] and crosslinking were established.[16–19] Since its emergence single chain polymer technology[16,20–23] has been guided and inspired by nature—not only to a gain deeper understanding of folding occurring in nature, e.g. in biopolymers and proteins and specifically the nature of their structure and activity relationships —but critically to replicate the interplay of structure and functionality from much simpler, more economical and easier to utilize building blocks (refer to Scheme 1 for key design considerations when using SCNPs in catalysis). The Zimmermann group made key contributions describing intramolecularly crosslinked dendrimers and their improved substrate binding mimicking a key-lock mechanism,[19,24,25] however, with the caveat of laborious synthesis. In 2013, the Lemcoff group collapsed a linear poly(cyclooctadiene) chain via rhodium moieties resulting in the first organometallic single chain nanoparticle as the term is used currently.[26] The following year they expanded on their work employing bimetallic SCNPs in cross coupling reactions which demonstrated enhanced activity due to confinement.[27] Catalytic SCNPs can combine the benefits of both homogeneous and heterogeneous catalysts such as homogeneous reaction conditions, improved recyclability, high activity, and potentially high substrate specificity. The folding of a linear chain via intramolecular crosslinking into an SCNP can give rise to the formation of local domains within the nanoparticle, which when decorated with catalytic moieties can afford 'catalytic pockets', analogous to enzymes.[28] While enhanced selectivity and specificity have been observed,[29] SCNPs require further development in order to replicate the catalytic capabilities of enzymes. SCNPs, however, offer opportunities not accessible with traditional enzymes, such as the ability to dynamically control catalysis via mild stimuli such as light or pH, arising from the bespoke tailoring of the SCNP scaffold. SCNPs can be equipped with functionality at all levels of design starting with the constituting monomers,[30] crosslinking chemistry[31] and morphological control of the final particle.[32] Enzymes do not offer the same degrees of freedom. For example, only a selection of metals occur naturally as biocatalytically active centres,[33] however, the choice of active metal is virtually unlimited for organometallic SCNPs. Analogous to enzymes, metal free organocatalysis is equally possible using SCNPs.[34,35] Dynamic catalytic properties have been realized in SCNPs by incorporating stimuli responsive catalytic groups, with the most commonly utilized being photo-redox catalysts and

[*] Dr. K. Mundsinger,[+] A. Izuagbe,[+] Dr. B. T. Tuten, Prof. C. Barner-Kowollik
School of Chemistry and Physics and Centre for Materials Science, Queensland University of Technology (QUT)
4000 Brisbane QLD (Australia)
E-mail: bryan.tuten@qut.edu.au
christopher.barnerkowollik@qut.edu.au

A. Izuagbe,[+] Prof. P. W. Roesky
Institute of Inorganic Chemistry, Karlsruhe Institute of Technology (KIT)
Engesserstrasse15, 76131 Karlsruhe (Germany)
E-mail: roesky@kit.edu

Prof. C. Barner-Kowollik
Institute of Nanotechnology (INT), Karlsruhe Institute of Technology (KIT)
Hermann-von-Helmholtz-Platz-1, 76344 Eggenstein-Leopoldshafen (Germany)
E-mail: christopher.barner-kowollik@kit.edu

[+] These authors contributed equally to this work.

photosensitizers.[36–38] A certain level of control over the catalysis is thus obtained via the interaction of the individual catalytic functionality and an external stimulus. Only a few examples exist where catalytic properties are controlled via changes in the SCNP morphology.[39] Controllable SCNP catalysis via on demand reversible structural changes not only entails the possibility of varying catalytic rates, but also enables tuneable substrate selectivity by changing the morphology of the catalytic site, allowing certain substrates while excluding others.[40] It is therefore of critical importance to determine the internal morphology of SCNPs for catalysis in order to elucidate how the morphological changes in SCNPs affect their catalytic activity. While several reviews summarising the advances in SCNP technology and catalysis exist,[20,23,40-52] in recent years there has been rapid progress in SCNP-based catalysis, yet there is no consolidated review of the latest findings. Herein, we close this critical gap in the literature.

Crosslinking chemistries to transform linear polymers into SCNPs are typically grouped into one of two classes, selective point folding and repeat unit folding. Selective point folding describes a linear polymer with folding points at predetermined positions that folds the entire chain ensemble into the same general SCNP geometry, while repeat unit folding results in a randomly folded SCNP derived from a randomly ordered linear copolymer with a statistical distribution of the folding points.[45] SCNPs can be further categorised into more specific folding techniques, i.e. homo-functional, hetero-functional and crosslinker mediated collapse.[55–57] Homo- and hetero-functional collapse relies on reactive partners situated along the polymer chain to induce collapse, while crosslinker mediated collapse is induced by an external crosslinking species. Chain collapse is most often performed at polymer concentrations below $1\ mg \cdot mL^{-1}$ to ensure that interchain crosslinking is minimised. However, a large number of synthetic techniques have been developed to overcome this scalability issue.[58,59] The polymer's collapse results in a decrease of its hydrodynamic volume, which can be observed by techniques such as size exclusion chromatography (SEC), dynamic light scattering (DLS) and diffusion ordered spectroscopy (DOSY).

A PhD graduate of Göttingen University, Germany, Christopher Barner-Kowollik joined the University of New South Wales in early 2000, becoming one of the co-directors of its Centre for Advanced Macromolecular Design in 2006. In 2008, he joined KIT, later establishing a DFG Centre of Excellence. He moved to QUT in 2017, founding QUT's Soft Matter Materials Laboratory. Over his 23-year career to date focussing on macromolecular photochemical processes, he supported highly collaborative large teams. His multi-award-winning research explores precision wavelength orthogonal, synergistic and antagonistic photochemical reactions and their application in macromolecular systems.

Peter W. Roesky obtained his doctoral degree from TU Munich in 1994. After postdoctoral work at Northwestern University, USA, he completed his habilitation at the University of Karlsruhe in 1999. He was appointed a full professor at the FU in 2001. In 2008, he became a full Professor at the Karlsruhe Institute of Technology (KIT). From 2013 to 2015, he served as Dean of the Faculty of Chemistry and Biosciences at KIT. His current research interests are synthetic inorganic and organometallic chemistry of s-block metals, silicon, phosphorus, gold, and lanthanides.

Bryan Tuten received his PhD in Materials Science and Engineering at the University of New Hampshire (USA, 2016) under the supervision of Prof. Erik Berda. Subsequently, he completed a postdoctoral research fellowship under the supervision of Prof Christopher Barner-Kowollik at the Karlsruhe Institute of Technology (Germany) and three years at Queensland University of Technology (Australia). Currently, Bryan is a Group Leader within the Soft Matter Materials laboratory at QUT exploring functional polymeric materials.

Aidan Izuagbe obtained his B.S degree from the Queensland University of Technology (QUT) in 2018 followed by his honors degree in 2019. He is currently a joint PhD candidate between QUT and the Karlsruhe Institute of Technology under the supervision of Prof. C. Barner-Kowollik (QUT/KIT) and Prof. P. W. Roesky (KIT). His current work focuses on the development of photo-responsive metal based single-chain nanoparticles.

Kai Mundsinger received his master's degree from the University of Stuttgart, Germany, and subsequently moved to the Queensland University of Technology, Australia, graduating with a PhD in 2021. Since then, he completed a postdoctoral fellowship with Prof Christopher Barner-Kowollik at Queensland University of Technology and is now working as a research fellow with Bryan Tuten. His research on functional polymer materials spans from microparticles and surface science to photochemistry.

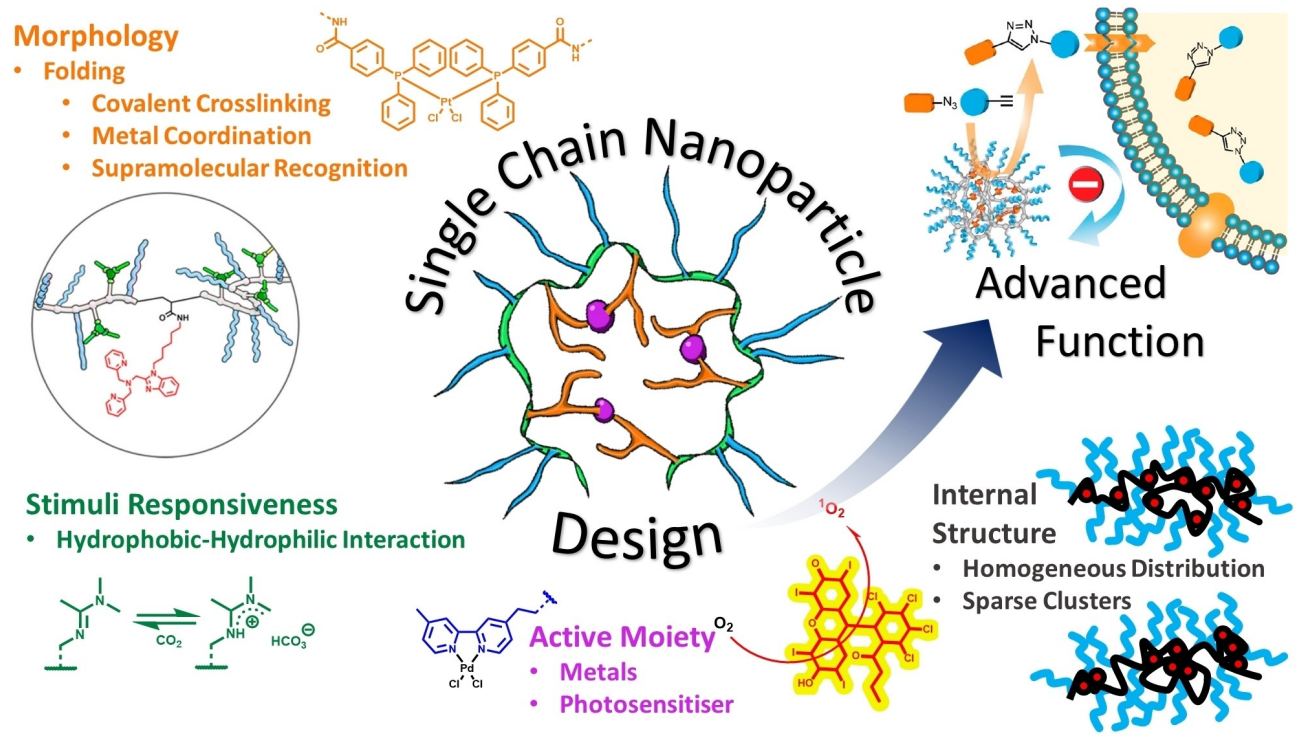

Scheme 1. Overview of single chain nanoparticle (SCNP) design considerations for catalysis. Elsevier.[53] American Chemical Society.[38,54]

Once formed, equipping an SCNP with catalytic properties is typically achieved via the introduction of catalytically active organometallic complexes. The primary coordinating structure of these complexes can be co-opted to additionally induce the collapse of the chain into an SCNP. A linear chain decorated with ligands as pendant groups can be crosslinked chelating a metal precursor with multiple pendant groups.[60–62] Metal complexes can further serve as purely catalytic elements, where chain collapse is induced via separate crosslinks allowing for the implementation of more diverse crosslinking strategies.[63,64] Characterization techniques used for small molecule metal complexes can also be applied to the comparable metallo-SCNPs, often with a notable decrease in resolution and accuracy owing to the disperse nature of the polymers they are embedded in. In some cases, defined metal complexes were synthesized in parallel to have model compounds for the polymer embedded complexes.[64,65] Techniques such as Fourier Transformed Infrared spectroscopy (FT-IR),[66] UV/Vis spectroscopy[67] and nucleus or ligand specific NMR techniques[65,68] are used for the determination of structural characteristic of metals embedded within an SCNP. The obtained data can be compared with small molecule metal complexes for a reliable assignment of the spectra. When employing NMR techniques, consideration should be taken when analysing SCNPs containing paramagnetic complexes, where significant line broadening can further complicate analysis.[69] Photoemission spectroscopic techniques such as energy dispersive X-ray spectroscopy (EDX) and X-ray photoelectron spectroscopy (XPS) also find use in the characterisation of metallic SCNPs providing elemental analysis.[70,71] In the constrained environments of SCNPs, metal coordination may not always match the theoretical coordination number. Thus, a Job plot analysis can be utilized to determine the binding stoichiometry of metal complexes within SCNPs.[61,72] The mismatch between metal and ligand often has noticeable impacts on catalysis. The overall influence that the polymer environment has on the distribution of catalytic sites within the internal structure of an SCNP is as important as the effect it has on the individual geometries of the catalytic sites. The polymeric environment provided by an SCNP allows for spatial confinement of catalytic sites embedded in the system. When appropriate compartmentalization of catalytic sites is achieved, an enhanced substrate selectivity and catalytic activity is possible. The self-confinement of catalytic sites and effects on catalytic performance are discussed in detail by Verde-Sesto et al.[46]

The ability to determine both the polymer morphology and the internal structure of catalytic SCNPs is of critical importance yet remains a challenging task. Characterization utilising Small Angle Scattering (SAS) techniques such as Small Angle Neutron Scattering (SANS) and Small angle X-ray Scattering (SAXS) is a popular method of elucidating the three dimensional conformations of SCNPs in solution, specifically the degree of compactness as well as the overall flexibility of the SCNP.[73,74] SANS techniques, often coupled with molecular dynamic simulations, have been used to categorise SCNPs in relation to two distinct morphologies, "sparse" and "globular" (Figure 1A). Pomposo et al. initially noted a linear Gaussian chain like behaviour of SCNPs collapsed in good solvents respective to the precursor

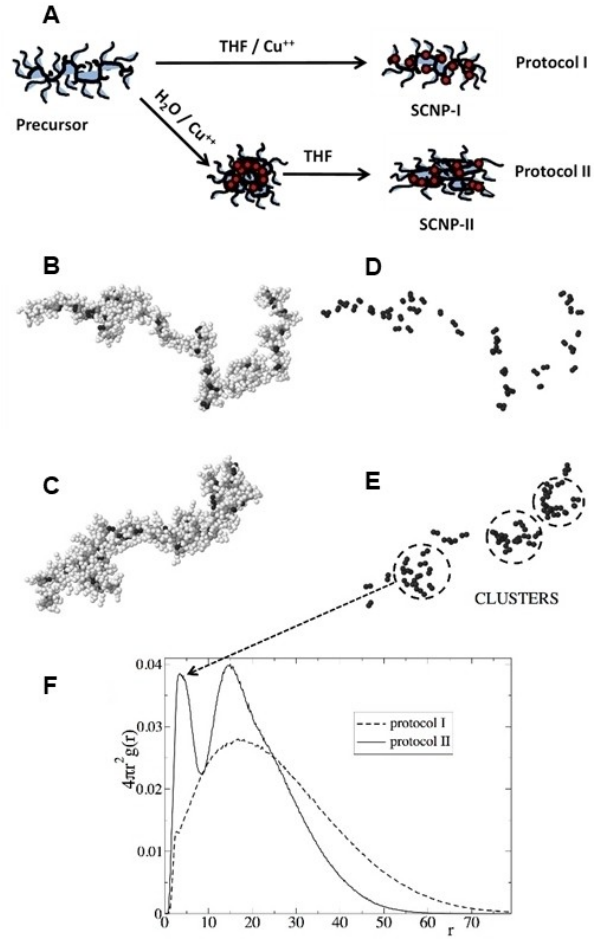

Figure 1. **A** Adapting the internal structure of metallo-folded SCNPs using amphiphilic random copolymers and two synthesis procedures involving non-selective (protocol I) and selective (protocol II) solvents. **B** and **C** Typical snapshot from MD simulations of a SCNPs synthesized via protocol I (B) and II (C) respectively. **D** and **E** only the catalytic sites are displayed, showing their spatial arrangement into clusters for protocol II (E). **F** Radial distribution function of the catalytic sites of the SCNPs synthesized by protocols I and II. Distance *r* is given in units of the bead diameter (refer to the text and Supporting Information of reference[53]). Elsevier.[53] Wiley.[78]

polymer. These SCNPs—coined "sparse SCNPs"—have a large number of locally compacted domains (Figure 1B–E).[75–77] SANS profiles of these SCNPs match those of proteins that bear a minimally ordered three dimensional conformation known as intrinsically disordered proteins (Figure 1F). Utilising the above process, the distribution of catalytic sites within an SCNP can be controlled by initially folding an amphiphilic block co-polymer in water and transferring the formed SCNP to THF.[78] A combined SAXS and molecular dynamic simulation (MDS) approach revealed clusters of catalytic sites compared to a more homogeneous distribution of catalytic sites along the chain when folding was exclusively performed in THF. In work recently completed by Patel et al., MD simulations were combined with machine learning to generate a large and diverse library of SCNPs simulated in good solvent conditions.[79] The study primarily explored the mean density of crosslinkable monomers throughout the chain and the 'blockiness' of the monomer distribution along the chain. These factors affect the overall morphology as well as the internal configuration of the subsequent SCNPs. It was found that high crosslinking densities consistently formed globular morphologies noting that blockiness had minimal impact. Conversely, when the crosslinking density is low, the generated morphologies are more akin to a sparse morphology and are far more susceptible to structural changes induced by different blockiness. The most significant morphological diversity was observed for polymers with low crosslinking density and medium to high blockiness. The variability suggests polymers in this regime are ideal for tailoring of the primary polymer sequence to yield specific morphologies. While understanding and observing the morphological properties of a catalytic SCNP is required in determining its function as a catalyst, direct substrate-SCNP interactions can also be exploited to elucidate more direct catalytic properties. Internal morphological properties of a catalytic SCNP can be indirectly elucidated by observing the binding and encapsulation of a substrate to catalytic sites within the SCNP.

Conversely, SCNPs folded from amphiphilic precursors in aqueous environments yield scattering profiles comparable to those of globular proteins such as enzymes. Such an SCNP has a far more compact morphology and a hydrophobic/hydrophilic core–shell structure possessing a relatively large centralised hydrophobic region.[80] Specifically, the Palmans team critically advanced such core/shell SCNPs with catalytic elements and hydrogen bonding benzene-1,3,5-tricarboxamide (BTA) units into enzyme mimetic SCNPs. Palmans and Meijer[38] established a versatile system of amphiphilic polymers that undergo non-covalent chain collapse in aqueous environments. The system was based on the controlled polymerization of *p*-pentafluorophenyl acrylate (PFPA), which can subsequently be functionalized in a stepwise fashion. Hydrophobic and hydrophilic pendant groups as well as a supramolecular recognition unit, i.e. tricarboxamide moieties, with amine functional handles were added to *poly*PFPA resulting in a polyacrylamide backbone carrying the desired pendant groups. In 2015, these authors embedded a Ru^{II} based catalyst within an amphiphilic block copolymer, which was subsequently folded in water incorporating the Ru^{II} catalyst into a central hydrophobic core facilitated by the self-stacking of BTA units, evidenced by circular dichroism (CD).[81] With the implementation of the hydrophobic pocket, substrate selectivity in alignment with varying substrate hydrophobicity was observed where the SCNP displayed enhanced selectivity towards hydrophobic substrates. The development of similar SCNP morphologies is limited in organic solvents, owing to the self-avoiding nature of polymers when placed in such good solvent environments, implying that more often a sparse configuration is observed as opposed to the more enzyme mimetic globular morphologies.

Nuclear Overhauser Effect Spectroscopy (NOESY) can be utilised to observe the location within an SCNP where a substrate binds, owing to the proximity of catalyst bound

substrate. Zimmerman et al. utilised Standard Transfer Difference (STD) spectroscopy, commonly used for elucidating small molecule ligand-protein binding, to evidence the substrate selectivity of SCNPs. STD analysis showed the increased encapsulation of hydrophobic alkyne substrates within a copper containing SCNP, when compared to a comparatively hydrophilic substrate. Further analysis with two dimensional (2D) NOESY highlighted the selective encapsulation of hydrophobic substrates within hydrophobic compartments formed by aliphatic side chains presents in the SCNP, evidenced by strong cross-peak signals between the substrate and SCNP bound alkyl chains.[82]

2. Current State of the Art in SCNP Catalysis

The Pomposo team investigated the effect of the catalytic site distribution in so-called 'clickase' SCNPs in 2021.[53] They crosslinked a linear poly(oligothylene glycol methacrylate)-co-(acetoacetoxy ethyl methacrylate) with Cu^{II} ions via two different pathways which resulted in an SCNP with a homogeneous distribution of catalytic sites (**SCNP1**) and an SCNP with local clusters of catalytic sites (**SCNP2**). Investigating the difference in catalytic performance via a fluorogenic click reaction between 9-(azidomethyl)anthracene and phenylacetylene demonstrated a remarkably increased activity of **SCNP2** (95 %) over **SCNP1** (65 %). Both SCNPs achieved significantly higher conversions than an equivalent small molecule catalyst (15 %). These findings highlight once more the importance of not only precise control, but analysis of the internal structure of SCNPs as chemically identical SCNPs can show significant differences in activity and possibly selectivity, due to differences in their internal morphology.

Patenaude, Berda and Pazicni[83] equipped a library of zinc porphyrin cores with poly(methyl methacrylate-co-anthracene methacrylate) (p(−co-AMMA) and p(MMA-co-AMMA-co-pentafluorophenyl methacrylate (PFPMA)) based polymers. The PFPMA moieties were subsequently used to equip the polymer with hexyl, isopropyl amide, and hydroxyethyl amide groups. The resulting polymer library was almost identical except for their functional groups that can possibly act as a secondary coordination sphere to ligands on the zinc core. All polymers in the library were also crosslinked via [4+4] cycloaddition of the anthracene moieties to yield an analogue library of SCNPs. When solutions of the polymers in DMF were treated with sodium cyanide their UV absorbance shifted, indicating formation of a Zn-porphyrin cyanide adduct. Over several hours the absorbance reverted, indicating loss of the cyanide ligand. Metal cyanides have been shown to react with DMF yielding hydrogen cyanide, carbon monoxide and metal dimethylamines.[84] The SCNPs exhibited faster reaction rates than their linear analogues suggesting spatial confinement is critical to the observed reaction. Furthermore, the hydrogen bonding SCNPs exhibited higher reactivities compared to the non-hydrogen bonding types. The most reactive system was the hydrogen bonding polymer with the highest steric demand, equipped with isopropyl amide (83 % conversion within 48 h versus 68 % for a small molecule species).

Over the last years, we have worked on incorporating various metals into SCNPs in mono- or bimetallic configurations, not only to introduce catalytic functionality, but to exploit metal coordination for crosslinking or enable tracing of the SCNP via photospectroscopy or even with the naked eye.[64,68,85] In contrast to previous studies containing Ir and Rh coordination via the same ligand, in a recent contribution, Knöfel et al.[68] prepared SCNPs with two disparate ligands binding either Pt^{II} or Eu^{III} ions via nitroxide mediated polymerization (NMP) of styrene, 4-(diphenylphosphino)styrene, and 4-(diphenylphosphine oxide)styrene and subsequent crosslinking via $Pt^{II}Cl_2$ scaffolds, intramolecularly chelated by two phosphine ligands. The phosphine oxide ligands did not bind to the Pt^{II} ions and were employed to coordinate to an Eu^{III} complex in a monodentate fashion, therefore not influencing the degree of crosslinking. According to ^{31}P NMR spectroscopy, the Pt^{II} ion was predominantly bound by phosphines in a *cis*-geometry, evidenced by the precursor having two *cis* chloride ligands leaving only two binding sites of that geometry available. Eu^{III} binding was evidenced via high field ^{1}H NMR spectroscopy. The heterobimetallic SCNPs were investigated regarding their catalytic properties for the amination of ally alcohols. The advantage over monometallic systems is associated with the fact that due to the Eu^{III} fluorescence, the presence of Eu^{III}/Pt^{II}-SCNP can readily be assessed via fluorescence spectroscopy and even with the naked eye (Figure 2C). Catalytic performance in the amination of allyl alcohol with aniline at 100 °C achieved quantitative conversions within 48 h with the monosubstituted amine constituting at least 80 % of the product. The catalytic SCNPs were readily retrieved via precipitation in methanol or, alternatively, removed via passing over silica.

In a similar fashion, Bohlen et al. improved the versatility of SCNPs by incorporating rare earth metals.[64] A styrene-based polymer carrying diphenylphosphine and benzoic acid pendant moieties (**P1**) was synthesized via NMP. The phosphine pendant groups were subsequently functionalised with $Au^{I}Cl$, while the benzoate groups were used to crosslink the polymer via coordination of a Y^{III} species (Figure 2A). IR spectroscopy confirmed the formation of an $yttrium^{III}$ benzoate complex, and compaction of the polymer was shown via SEC (25 % decrease in apparent molecular weight). The Au^{I}/Y^{III}-SCNP was investigated with respect to its performance in catalysing the hydroamination of aminoalkynes against $[AuCl(PPh_3)]$ and a linear Au^{I}-polymer as benchmarks. For a substrate with high steric demand, the performance of all three catalytic species was identical, achieving near quantitative conversion (96–98 %) within 4 h at 20 °C and 2 mol-% Au^{I} catalyst loading, and quantitative conversion within 24 h. For substrates with lower steric demand and therefore less driving force towards ring closure, the linear polymer (83 %) outperformed the small molecule catalyst (58 %), while Au^{I}/Y^{III}-SCNPs exhibited lower conversion (41 %) than the small molecule catalyst after 4 h. Whether the discrepancy between linear Au^{I}-polymer and Au^{I}/Y^{III}-SCNPs was due to compaction or

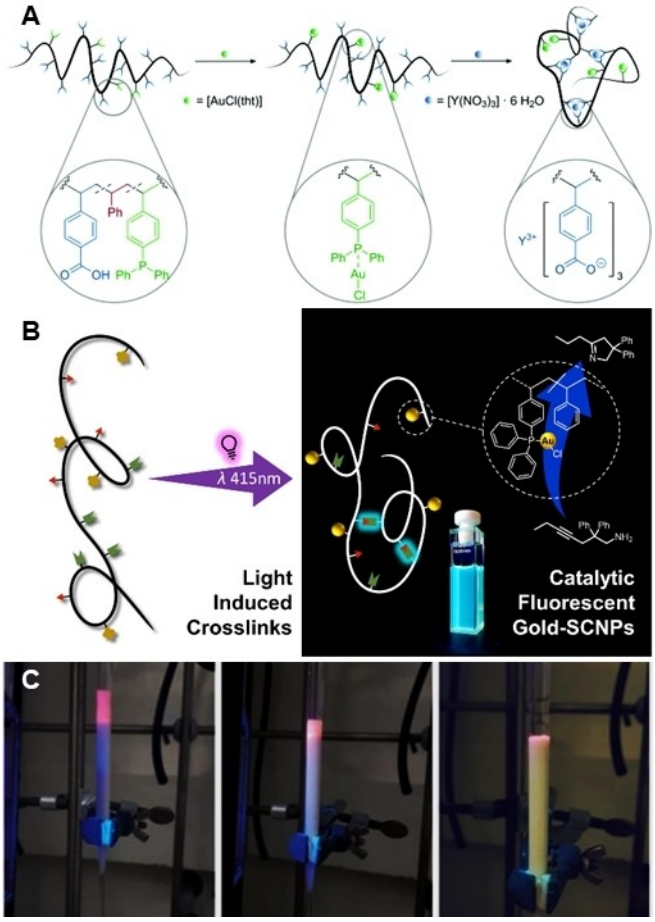

Figure 2. **A** Au^{I} functionalization of **P1** using [AuCl(tht)] (tht = tetrahydrothiophene) and subsequent folding of the obtained metallopolymer P1-Au^{I} with $[Y(NO_3)_3]\cdot 6\ H_2O$. The metal species coordinate orthogonally to the respective ligands in the polymer, affording well-defined catalytically active Au^{I}/Y^{III}-SCNPs. Royal Society of Chemistry.[64] **B** Visible light folded SCNPs exhibiting fluorescent crosslinks and catalytically active Au moieties. American Chemical Society.[85] **C** Exemplary separation of the Eu^{III}(tta)/Pt^{II}-SCNPs (tta = 2-thenoyltrifluoroacetonate) via a short column chromatography (neutral aluminium oxide; acetone) subsequent to the catalytic reaction. Royal Society of Chemistry.[68]

presence of Y^{III} was not explored. The Au^{I}/Y^{III}-SCNP was recovered via dialysis with minimal observable degradation (established via SEC and NMR spectroscopy) and subjected to a further catalytic cycle where the SCNPs were demonstrated to be active, albeit at lower rates. Maag et al.[85] revisited the concept of facile tracking of the SCNP via photophysical methods, in this case fluorescence. A styrene-*co*-(bromomethyl)styrene based linear polymer carrying a protected phosphine ligand ($S{=}PPh_2Sty$) was synthesized via NMP. The copolymer was subsequently modified with an alkyne and *o*-methyl benzaldehyde (*o*-MBA) via SN2 post-polymerization modification. Upon irradiation with 415 nm light, the *o*-MBA underwent a [4+2] cycloaddition with the alkyne groups forming profluorescent crosslinks, thereby compacting the linear polymer into an SCNP (Figure 2B). Under acidic conditions, the crosslink aromatizes and exhibits blue fluorescence. Subsequently, the protected phosphine ligand was deprotected and functionalized with catalytically active Au^{I}. Compared to the labile Eu^{III} system, the aromatic crosslink provides a readily accessible fluorescent alternative to lanthanides with greater tolerance to reaction conditions, enabling recyclability and tracking of Au^{I}-SCNP. These studies highlight the large potential SCNPs offer to the field of catalysis as they demonstrate the enhanced chemical activity of homogeneous metal catalysts, while simultaneously providing the ease of separation found in heterogeneous systems. In addition, SCNPs offer the ability to incorporate combinations of metals that would otherwise interfere with their respective functions, opening an avenue for multiple substrate transformations in a single environment.

In 2022, the Palmans group expanded on their previous work constructing Pd^{II} amphiphilic nanoparticles for pro-drug activation.[86] In an effort to produce Pd^{II} functionalized SCNPs, Sathyan et al. equipped *poly*PFPA with hydrophilic Jeffamine pendant groups, hydrophobic *n*-dodecyl groups and BTA units. Additionally, pendant triphenylphosphine (TPP) or bipyridine pendant moieties were added to complex Pd^{II} ions (Figure 3A). A library of polymers was synthesised utilizing varying amounts of TPP and bipyridine ligands. Due to a small amount of aggregation evidenced by DLS, the authors restricted themselves to describing the nanoparticles as polymeric nanoparticles instead of SCNPs. The Pd-nanoparticles were benchmarked against the corresponding Pd complex in depropargylation reactions of profluorescent substrates. An increase in reaction rate was correlated with substrate hydrophobicity, while the polymer composition only had a minor effect as long as it exhibited a hydrophobic interior (Figure 3B). Increased fluorescence quenching over time suggested accumulation of the products in the hydrophobic interior of the particles. Comparison between catalytic rates of the Pd salts and the nanoparticles in Dulbecco's Modified Eagle Medium (DMEM) demonstrated that when retained within the hydrophobic pocket of a nanoparticle (NP), the catalytic sites were protected from deactivating species thereby retaining their some catalytic activity, while free Pd salts were completely deactivated. Encapsulating Pd salts and complexes within a collapsed polymer did not follow this same trend, instead—due to the lack of covalent linkages between catalyst and polymer—almost complete catalyst deactivation was observed, highlighting the importance of a covalent linkage in complex media. Investigation of pro-drugs of variable hydrophobicity resulted in similar outcomes, where hydrophilic pro drugs were successfully deprotected by the NP used in equimolar amounts compared to small molecule Pd salts that failed to achieve full conversion. More hydrophobic pro-drugs failed to be efficiently activated due to the pro-drug/activated drug accumulating within the Pd-NP. Doxorubicin-based pro-drugs were more efficiently activated by the Pd complex compared to the Pd-NP, probably due to a combination of their easily cleavable protecting groups and high hydrophilicity. These findings highlight that covalent attachment of Pd complexes is necessary. Efficiency in this case correlates with hydrophobicity of the substrate. In 2023

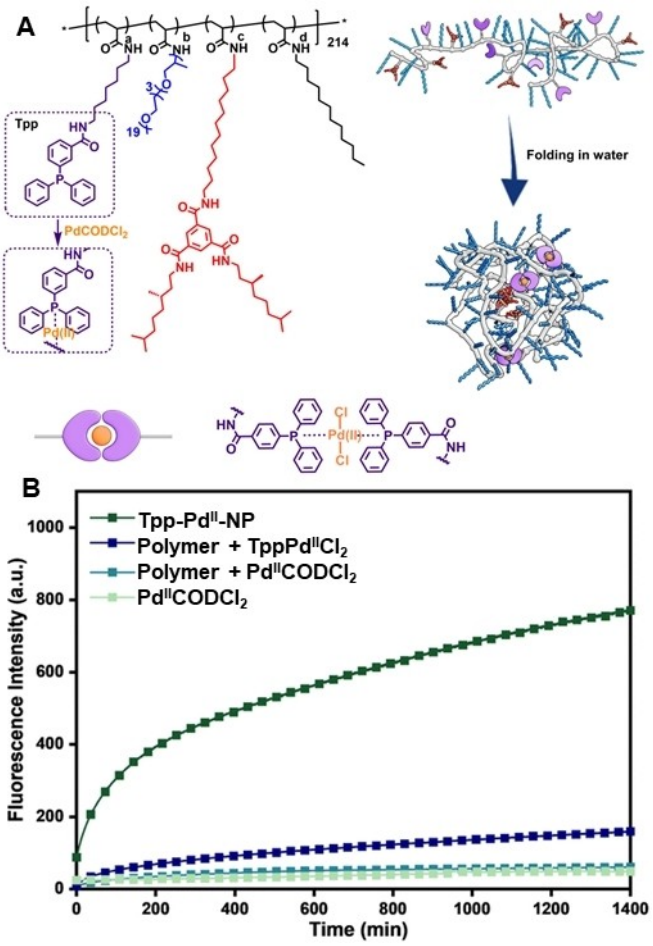

Figure 3. **A** Depiction of the structures of amphiphilic copolymers bearing TPP (**Tpp-Pd^{II}-NP**) ligands for the complexation with Pd^{II} ions mediating the depropargylation reactions of propargyl protected dyes. **B** Depropargylation of propargyl capped rhodamine dye (pro-rho) in Dulbecco's Modified Eagle Medium catalyzed by **Tpp-Pd^{II}-NP**, free [TppPd^{II}Cl$_2$] complex in the presence of polymer, [Pd^{II}(COD)Cl$_2$] in the presence of polymer and just [Pd^{II}(COD)Cl$_2$]. Royal Society of Chemistry.[86]

Sathyan et al. generated polymer nanoparticles comprising dodecyl and Jeffamine pendant groups and used these to encapsulate dirhodium^{II} carboxylate complexes via chain collapse in water and matching of the polarity of suitable complexes to their hydrophobic interior.[87] Complexes with hydrophobic ligands were incorporated with efficiencies greater than 97 %, while a hydrophilic ligand complex was only incorporated with 50 % efficiency. As discussed above, the formed particles consisted of polymer chain aggregates, indicated by a size increase in DLS, hence not termed SCNP, but "amphiphilic polymer nanoparticles". The encapsulated complexes were benchmarked in NH carbene insertion reactions and a phthalimide-adamantyl functionalized complex was found to be the most active. Catalysis performed initially in DMEM and DMEM with foetal bovine serum (FBS) was exported to living cells by incubating HeLa cells with polymer encapsulated rhodium catalyst and profluorescent substrates yielding fluorescent benzoquinoxalines. A fluorescence turn-on was observed within 1.5 h, which did not occur in the control experiments. The catalysis likely occurs extracellularly, however, and the fluorescent product subsequently crosses the cell membrane as the employed nanoparticles are known to exhibit very slow cell uptake.[88] Furthermore, the active nanoparticles were used to form cytotoxic compounds at low catalyst loadings evidencing their potential in biomedical applications.

The Zimmermann group previously reported enzyme-like behaviour of copper containing SCNPs in copper catalyzed alkyne-azide cycloaddition (CuAAc) reactions (Figure 4A),[82,89] and recently Chen et al.[54] expanded on these copper-containing 'clickase' SCNPs with hydrophobic core and hydrophilic—quart ammonium shells (**Cu^{I}-SCNP-NR$_4^+$**). After polymerization of pentafluorophenylacrylate, the linear polymer was functionalized with 6-aminohexanoic acid, 3-azidopropylamine and MePEG$_{1000}$ and subsequently crosslinked in water via CuAAc resulting in BTA like ligands (Figure 4B). The water-soluble exterior via PEGylation (**Cu^{I}-SCNP-PEG**) exhibited no electrical charges as indicated by lower zeta potential and minimal protein binding to bovine serum albumin (BSA). Comparison of click reactions between a profluorescent coumarin substrate, 3-azido-7-hydroxycoumarin (**Az1**), and small molecule alkynes or BSA bound alkynes showed a 60-fold preference of the PEG shell SCNP for small molecules over the protein bound alkyne, suggesting that the PEG exterior successfully prohibits the active sites contacting proteins.

Furthermore, the applicability of **Cu^{I}-SCNP-PEG** in protein binding studies was demonstrated by comparing the fluorescence turn-on by reacting six nonbinding and one binding alkyne to **Az1** in the presence and absence of carbonic anhydrase II (CA) (Figure 5A). The reactivity towards the binding substrate was significantly diminished in

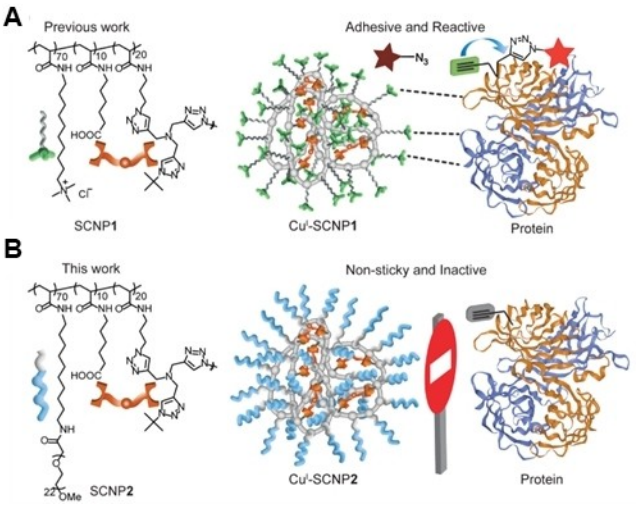

Figure 4. Illustrations of the two Cu^{I} based SCNPs. **A** charged side-chain, copper containing SCNP (**Cu^{I}-SCNP-NR$_4^+$**). **B** polyethylene glycol sidechain, copper containing SCNP (**Cu^{I}-SCNP-PEG**). American Chemical Society.[54]

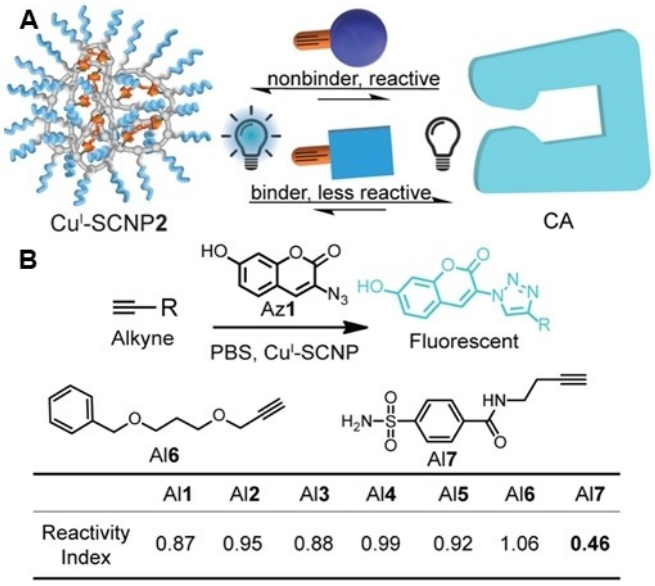

	Al1	Al2	Al3	Al4	Al5	Al6	Al7
Reactivity Index	0.87	0.95	0.88	0.99	0.92	1.06	**0.46**

Figure 5. **A** Illustration of the competitive binding of carbonic anhydrase II (CA) and **Cu^I-SCNP-PEG**, only free substrates can interact with the nanoparticle. **B** Reactivity indices of tested substrates. Numbers close to 1 indicate no protein binding, numbers smaller than 1 indicate protein binding. Only Al6 (non-inhibiting) and Al7 (known CA inhibitor) are depicted here, for Al1–5 refer to the original publication. American Chemical Society.[54]

the presence of CA, while the non-binding substrates retained their activity.

Using **Cu^I-SCNP-NR$_4^+$** in combination with **Cu^I-SCNP-PEG** allowed to differentiate even further by using both SCNPs as a dual logic gate. Nonbinding substrates are accessible to both SCNPs, substrates that bind leaving alkynes on the surface of the protein are accessible to only **Cu^I-SCNP-NR$_4^+$** and substrates that are completely taken into the protein, burying the alkyne within its structure, inaccessible to either SCNP (Figure 5B). These findings were translated into a fluorogenic assay to test ligands as proteolysis targeting chimeras. Ligands with two protein binding moieties equipped with adjacent alkynes can be examined with the aforementioned dual logic gate in respect to their protein binding properties of either binding moiety.

Given the weak protein binding, the cellular uptake of **Cu^I-SCNP-PEG** was assessed via labelling of the SCNP with Cyanine 5 dye and found to be minimal, however, exhibiting significant cytotoxicity above 8 μM. This enabled the authors to perform CuAAc in the extracellular medium of HeLa cells. A library of six alkynes and ten profluorescent azides were examined and a gradual increase of fluorescence in the HeLa cells was observed, indicating uptake of the reaction products into the cells. These findings illustrate that SCNPs are not only potent catalysts for bioorthogonal reactions but can themselves be bioorthogonal with potential applications in drug screening. The surface charge of the SCNP, or lack thereof, determines the interaction with proteins enabling the presence of copper in biological systems without inducing cytotoxicity. Non-protein binding SCNPs allow catalysis in cellular environments, enabling for example localized, on demand activation of drugs. Furthermore, the combination of protein binding and non-binding SCNPs created a dual logic gate which can be used to study ligand-protein binding.

A similar approach by Xiong et al.[90] exploited the post-functionalization of linear polymers based on pentafluorophenyl acrylate polymerized via RAFT. Subsequently, the pentafluorophenyl groups were substituted with 10-trimethylammonium-1-decylamine and either 6-(2-naphtyloxy)-1-hexylamine or hexylamine. The quaternary ammonium side chains provided water solubility, while the aliphatic side chains allowed folding in aqueous solution and provided a hydrophobic interior. Bis(*tert*-butyltriazolyl) ligands carrying naphtyloxyhexyl and hexyl side chains were used to complex copper sulfate in the presence of the polymers. The non-covalent incorporation of the ligands into the polymers was studied via NOESY NMR spectroscopy and new cross resonances due to interactions of the polymer backbone, side chains and ligands were observed. Using DOSY, the ligand was found to be partially bound due to an average diffusion coefficient between the small molecule and polymer species. Different ligand side chains were tested to investigate their influence on ligand binding and catalytic activity. An acid side chain was found to perform the best, presumably due to being negatively charged and exhibiting strong interactions with the positively charged polymers. All ligand-polymer systems outperformed the small molecule catalyst. Further investigations with ruthenium catalysts equipped with hydrophobic side chains indicated increased activity due to those catalysts being driven into the hydrophobic interior of the particles. The presented system provides a library of building blocks that can be combined in a modular fashion according to the desired function.

The same polymer architecture was utilized by Garcia et al.[91] to generate water soluble SCNPs equipped with a ruthenium complexing ligand in conjunction with β-galactosidase. To obtain ruthenium containing SCNPs (**Ru-SCNP**), the quinoline functionalized prepolymer was treated with $[CpRu(MeCN)_3]PF_6$. Binding was evidenced via shifted ^{1}H NMR resonances of the ligating group and quantified via UV/Vis. After determining the critical micelle concentration (CMC), the **Ru-SCNP** was benchmarked against a small molecule ruthenium catalyst at concentrations below, at, and above the CMC. Reaction rates of allylcarbamate cleavage in phosphate buffered saline (PBS), releasing a fluorescent coumarin, increased with increased ruthenium concentration, highlighting that the **Ru-SCNP** outperformed the small molecule catalyst significantly. The **Ru-SCNP** also showed significantly higher activity than the small molecule in DMEM and DMEM with glutathione (GSH). In HeLa cell lysate, however, the small molecule catalyst showed slightly higher initial rates and similar conversions after 20 min as compared to the **Ru-SCNP**. The lower activity is potentially due to unfolding of the polymer and interactions of the polymer and compounds from the cell lysate. **Ru-SCNP** was further utilized in tandem catalysis with β-galactosidase, with the **Ru-SCNP** deprotecting an allylcarbamate phenyl carbonate protected galactopyranoside (MUG) linked to

coumarin, subsequently β-galactosidase cleaves off the fluorescent coumarin. The **Ru-SCNP** system achieved conversions of 69 % in PBS and 38 % in DMEM, while the small molecule ruthenium catalyst only exhibited conversions under 2 %. The SCNP protects the active metal species from buffer solutions and retains its activity in the presence of enzymes without interfering with the enzymatic reaction while the ruthenium of the small molecule catalyst is exposed to any compound in the media and potentially poisoned. The lack of covalent crosslinks potentially limits its application in more complex media like cell lysate.

Zwitterionic sulfobetaine methacrylate and fluorinated methacrylate copolymers were employed by Zeng *at al.*[92] They explored a plethora of monomer ratios and polymer sizes and characterised how these affect the single chain collapse in water. The ratios that resulted in SCNPs were used in conjunction with enzymes, first horseradish peroxidase (HRP) and subsequently HRP in tandem with glucose oxidase (GO), to oxidize 4-amino benzenesulfonic acid into azobenzene disulfonic acid (Figure 6A–D). Similar to Chen et al.[54] these authors found that charged side chains enable protein binding, while non-charged pendant groups do not bind to proteins. SCNPs with charged pendant groups clustered on the protein surface, stabilizing it and increased the enzyme activity fivefold. Linear zwitterionic polymers had a similar effect, stabilizing the enzyme and increasing its activity fourfold. These findings corroborate reports from the Zimmerman group and further evidenced the role charges play in protein binding, even when the SCNP is not the active component but supports an active enzyme.

We recently exploited the amphiphilic nature of poly(ethylene glycol) methacrylate (PEGMA) based SCNPs,[93] which was demonstrated earlier by Hoffmann et al.[94] PEGMA was copolymerized with glycidyl methacrylate via RAFT polymerization and subsequently crosslinked via multifunctional thiol-epoxide ligation and functionalized with Rose Bengal (**RB**) in a one-pot reaction, affording SCNPs with a hydrophilic shell and hydrophobic photocatalytic regions (**RB-SCNP**) (Figure 7A). **RB-SCNP** outperformed the small molecule photosensitizer Rose Bengal at the same concentration of photoactive moiety in the oxidation of fatty acids by a factor of three. The core of the SCNP provides a hydrophobic environment with a higher local concentration of the substrate at the location of singlet oxygen generation. The lifetime of the photosensitizer was not significantly increased, evidenced by the similar timescale of decoloration of solutions of **RB-SCNP** and small molecule **RB**. The association of fatty acid and **RB-SCNP** was further investigated via molecular dynamics (MD) simulations and contact between the **RB** moieties and oleic acid was found to occur for 5 % of the simulated trajectory of oleic acid. The nature of the catalytic pockets was also probed via MD simulations and found to be of a transient

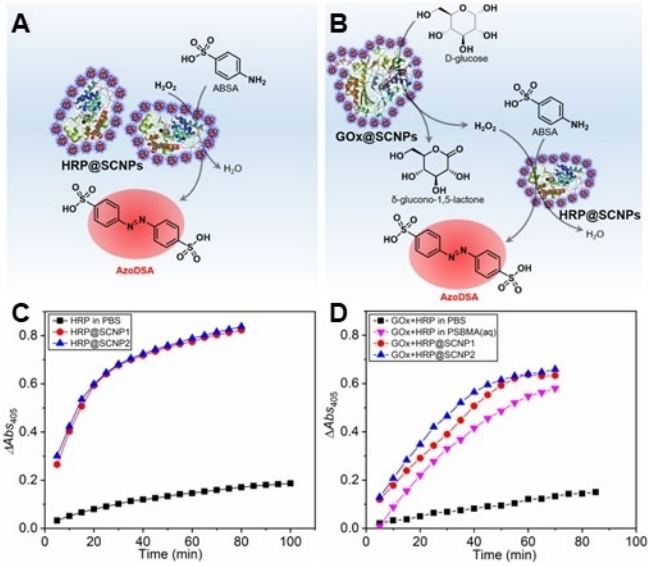

Figure 6. **A** Illustration of SCNP stabilised horse radish peroxidase (HRP@SCNP) catalysing 4-amino benzene sulfonate (ABSA) into an azobenzene in the presence of hydrogen peroxide. **B** Schematic illustration of a cascade reaction between SCNP stabilised glucose oxidase GOx@SCNP and HRP@SCNP. **C**,**D** Catalytic activity of the SCNP stabilised enzymes compared to the free enzymes in solution. American Chemical Society.[92]

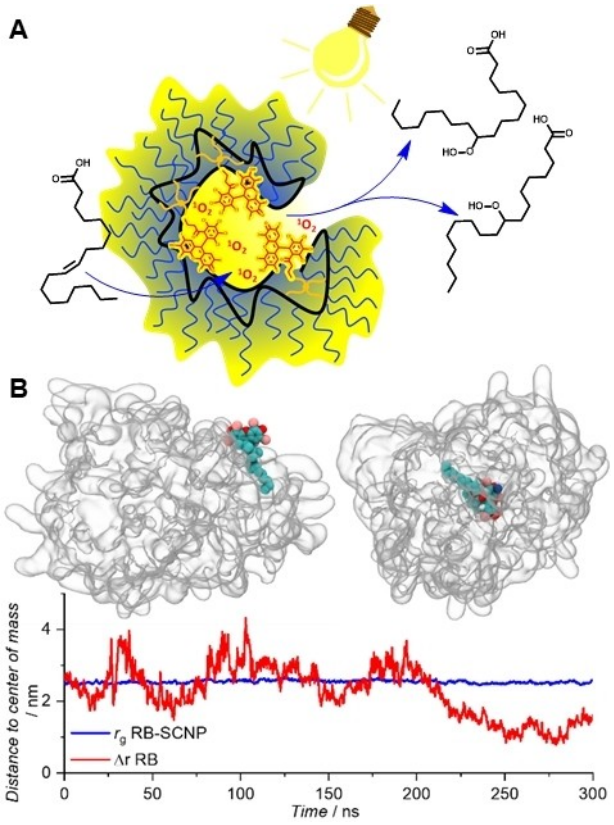

Figure 7. **A** Hydrophobic molecules (oleic acid) are driven into the hydrophobic region, oxidized under irradiation via generation of singlet oxygen and the products are subsequently expelled. **B** Snapshots of the position of one Rose Bengal (**RB**) moiety within the Rose Bengal functionalized single-chain nanoparticle (**RB-SCNP**) at two frames (98.6 ns and 279.4 ns) during the simulation in acetonitrile with 10 % water. Wiley.[93]

nature. The active **RB** moieties were found to be encapsulated within the SCNP for approximately 60 % of the time and on the SCNP surface for close to 40 % of the time (Figure 7B). This work highlights the scope for designing functional SCNPs based on commercially available starting materials via simple transformations and illustrates the potential SCNPs offer to transform non-catalytic processes into pseudo-catalytic reactions with high turnover numbers.

A recent example of switchable catalysis via application of external stimuli is explored by Liu et al.[95] These authors generated SCNPs via RAFT polymerization of dodecyl acrylamide carrying amidine and dodecyl acrylamide decorated with chiral salen Fe^{III} complexes (Fe(salen)). A plethora of ratios of amidine pendant groups and Fe(salen) was screened and evaluated regarding their behaviour in aqueous solution. The amidine pendant groups can bind CO_2 by forming bicarbonate salts making it more hydrophilic. Neat amidine groups are relatively hydrophobic and the resulting polymers aggregate in aqueous solution. Upon sparging the solutions with CO_2, the amidine becomes hydrophilic, aggregation ceases and the linear chains become solvated. Between a ratio of 26:1 and 72:1 amidine to Fe(salen), the linear chains collapsed into SCNPs in an aqueous environment. When sparging the solutions with nitrogen, the CO_2 is displaced, the amidines return to their hydrophobic nature and the polymers desolvate and can subsequently be recovered by centrifugation. Three SCNPs, with amidine to Fe(salen) ratios of 155:6, 202:4 and 218:3 were evaluated regarding their activity in enantioselective thiol-Michael additions, which is typically not possible in aqueous systems due to water coordinating to the Fe complex. All three SCNPs exhibited near quantitative conversion and high enantiomeric excess (99 % in the case of 202:4) at 1 mol % catalyst loading, outperforming the group's previous catalytic SCNP that required 3 mol % catalyst loading for similar conversion. Furthermore, the introduction of an imidazolium linker proved to be critical for the catalytic activity as an equivalent SCNP with Fe(salen) bound without the imidazolium performed considerably worse. These results fuse findings from other groups by combining an advanced SCNP design with sophisticated metal complexation and stimulus responsive polymer morphology and therefore constitute one of the most advanced single chain systems presented to date.

3. Perspective and Outlook

While steady progress has been made, SCNPs still face many challenges before they can realise their full potential, including in the herein discussed realm of catalysis. Currently, catalysis in SCNPs is largely achieved by 'polarity matching' between the substrate and the inside of the catalytically active SCNP, enabling the substrate to effectively enter the inside of the SCNP and increase the local substrate concentration in direct vicinity of the active moiety. While such an approach is certainly valuable, it is not driven by the bespoke key-lock principles that natural enzymes exploit for highly efficient catalysis. Thus, there is ample scope for SCNP designs employing sequence-defined polymers—polymers that have a defined sequence of their repeat units and feature uniform dispersity—and fold into a pre-determined geometry tailor-made for a specific substrate. We argue that key barries to implementing key-lock catalytic principles are currently not our ability to generate sequence-defined polymers—which is well-developed—but rather the theoretical understanding of how these polymers need to be designed and folded. Future progress will critically depend on the close collaboration of synthetic polymer chemists with theoreticians in the field of molecular dynamic simulations as well as biochemists. Fusing these fields will potentially allow to generate SCNP-based synthetic catalysts that feature superior stability over their natural counterparts, while demonstrating similar catalytic turnover rates.

A further critical frontier for next generation catalytically active SCNPs is to equip them with the ability to on-demand control catalysis via changes in their internal morphology due to external triggers. Access to the catalytic pocket or its polarity can be tuned by a post-compaction of the SCNP by external triggers, which may allow to temporally control catalytic activity. One highly attractive trigger to achieve external control over catalytic activity is light—ideally light in the visible light range—as a compaction of the morphology may be possible via the use of photo-switches that are present in the main chain of the polymer constituting the SCNP.[96] Other triggers are also conceivable such as temperature—exploiting the behaviour of thermoresponsive polymers—or pH changes.

Finally, it is a matter of priority to expand the substrate scope that catalytically active SCNPs can address, as it is currently still relatively limited compared to the plethora of small molecule catalysts. In this context, is it is important to remember why SCNPs are attractive catalysts: They constitute a bridge between homogeneous and heterogeneous catalysis, fusing the advantages of both techniques, while holding the potential to catalyze reactions with high selectivity under demanding reaction conditions.

Acknowledgements

C.B.-K. acknowledges the Australian Research Council (ARC) for funding in the context of a Laureate Fellowship enabling his photochemical research program. B.T. acknowledges the ARC for funding a DECRA fellowship. We thank Prof Megan O'Mara and Dr Lily Wang for the 3D render used in the ToC Figure. Open Access publishing facilitated by Queensland University of Technology, as part of the Wiley - Queensland University of Technology agreement via the Council of Australian University Librarians.

Conflict of Interest

The authors declare no conflict of interest.

Data Availability Statement

The data that support the findings of this study are available from the corresponding author upon reasonable request.

Keywords: Catalysis · Polymer Characterization · Polymer Chemistry · Polymer Morphology · Single Chain Nanoparticles (SCNPs)

[1] H. Staudinger, *Ber. Dtsch. Chem. Ges. B Ser.* **1920**, *53*, 1073–1085.
[2] P. Moseley, *Immunopharmacology* **2000**, *48*, 299–302.
[3] M. Wegner, *SOX Transcr. Factors* **2010**, *42*, 381–390.
[4] G. Cooper, *The Cell: A Molecular Approach*, Sinauer Associates, Sunderland, MA, **2000**.
[5] M. Raynal, P. Ballester, A. Vidal-Ferran, P. W. N. M. van Leeuwen, *Chem. Soc. Rev.* **2014**, *43*, 1734–1787.
[6] W. Kuhn, G. Balmer, *J. Polym. Sci.* **1962**, *57*, 311–319.
[7] J. E. Martin, B. E. Eichinger, *Macromolecules* **1983**, *16*, 1350–1358.
[8] Von. W. Kuhn, H. Majer, *Makromol. Chem.* **1956**, *18*, 239–253.
[9] G. Allen, J. Burgess, S. F. Edwards, D. J. Walsh, *Proc. R. Soc. Lond. Math. Phys. Sci.* **1997**, *334*, 453–463.
[10] J. E. Martin, B. E. Eichinger, *Macromolecules* **1983**, *16*, 1345–1350.
[11] M. Antonietti, H. Sillescu, *Macromolecules* **1986**, *19*, 798–803.
[12] M. Antonietti, H. Sillescu, M. Schmidt, H. Schuch, *Macromolecules* **1988**, *21*, 736–742.
[13] K. Matyjaszewski, J. Xia, *Chem. Rev.* **2001**, *101*, 2921–2990.
[14] N. Zhang, S. R. Samanta, B. M. Rosen, V. Percec, *Chem. Rev.* **2014**, *114*, 5848–5958.
[15] C. J. Hawker, K. L. Wooley, *Science* **2005**, *309*, 1200–1205.
[16] E. Harth, B. V. Horn, V. Y. Lee, D. S. Germack, C. P. Gonzales, R. D. Miller, C. J. Hawker, *J. Am. Chem. Soc.* **2002**, *124*, 8653–8660.
[17] C. W. Bielawski, R. H. Grubbs, *Prog. Polym. Sci.* **2007**, *32*, 1–29.
[18] A. E. Cherian, F. C. Sun, S. S. Sheiko, G. W. Coates, *J. Am. Chem. Soc.* **2007**, *129*, 11350–11351.
[19] N. G. Lemcoff, T. A. Spurlin, A. A. Gewirth, S. C. Zimmerman, J. B. Beil, S. L. Elmer, H. G. Vandeveer, *J. Am. Chem. Soc.* **2004**, *126*, 11420–11421.
[20] T. Terashima, T. Mes, T. F. A. De Greef, M. A. J. Gillissen, P. Besenius, A. R. A. Palmans, E. W. Meijer, *J. Am. Chem. Soc.* **2011**, *133*, 4742–4745.
[21] J. B. Beck, K. L. Killops, T. Kang, K. Sivanandan, A. Bayles, M. E. Mackay, K. L. Wooley, C. J. Hawker, *Macromolecules* **2009**, *42*, 5629–5635.
[22] E. J. Foster, E. B. Berda, E. W. Meijer, *J. Am. Chem. Soc.* **2009**, *131*, 6964–6966.
[23] A. P. P. Kröger, J. M. J. Paulusse, *J. Controlled Release* **2018**, *286*, 326–347.
[24] J. B. Beil, N. G. Lemcoff, S. C. Zimmerman, *J. Am. Chem. Soc.* **2004**, *126*, 13576–13577.
[25] S. C. Zimmerman, I. Zharov, M. S. Wendland, N. A. Rakow, K. S. Suslick, *J. Am. Chem. Soc.* **2003**, *125*, 13504–13518.
[26] S. Mavila, C. E. Diesendruck, S. Linde, L. Amir, R. Shikler, N. G. Lemcoff, *Angew. Chem. Int. Ed.* **2013**, *52*, 5767–5770.
[27] S. Mavila, I. Rozenberg, N. G. Lemcoff, *Chem. Sci.* **2014**, *5*, 4196–4203.
[28] J. A. Pomposo, A. J. Moreno, A. Arbe, J. Colmenero, *ACS Omega* **2018**, *3*, 8648–8654.
[29] A. Sanchez-Sanchez, A. Arbe, J. Colmenero, J. A. Pomposo, *ACS Macro Lett.* **2014**, *3*, 439–443.
[30] J. T. Offenloch, J. Willenbacher, P. Tzvetkova, C. Heiler, H. Mutlu, C. Barner-Kowollik, *Chem. Commun.* **2017**, *53*, 775–778.
[31] S. Thanneeru, J. K. Nganga, A. S. Amin, B. Liu, L. Jin, A. M. Angeles-Boza, J. He, *ChemCatChem* **2017**, *9*, 1157–1162.
[32] G. Li, F. Tao, L. Wang, Y. Li, R. Bai, *Polym. Ion. Liq.* **2014**, *55*, 3696–3702.
[33] S. Mounicou, J. Szpunar, R. Lobinski, *Chem. Soc. Rev.* **2009**, *38*, 1119–1138.
[34] R. Lambert, A.-L. Wirotius, D. Taton, *ACS Macro Lett.* **2017**, *6*, 489–494.
[35] J. J. Piane, S. Huss, L. T. Alameda, S. J. Koehler, L. E. Chamberlain, M. J. Schubach, A. C. Hoover, E. Elacqua, *J. Polym. Sci.* **2021**, *59*, 2867–2877.
[36] J. J. Piane, L. E. Chamberlain, S. Huss, L. T. Alameda, A. C. Hoover, E. Elacqua, *ACS Catal.* **2020**, *10*, 13251–13256.
[37] D. Kilic, C. Pamukcu, D. K. Balta, B. A. Temel, G. Temel, *Eur. Polym. J.* **2020**, *125*, 109469.
[38] Y. Liu, T. Pauloehrl, S. I. Presolski, L. Albertazzi, A. R. A. Palmans, E. W. Meijer, *J. Am. Chem. Soc.* **2015**, *137*, 13096–13105.
[39] X. Chen, Z. Chen, L. Ma, *Polym. Chem.* **2022**, *13*, 959–966.
[40] H. Rothfuss, N. D. Knöfel, P. W. Roesky, C. Barner-Kowollik, *J. Am. Chem. Soc.* **2018**, *140*, 5875–5881.
[41] C. K. Lyon, A. Prasher, A. M. Hanlon, B. T. Tuten, C. A. Tooley, P. G. Frank, E. B. Berda, *Polym. Chem.* **2015**, *6*, 181–197.
[42] M. Gonzalez-Burgos, A. Latorre-Sanchez, J. A. Pomposo, *Chem. Soc. Rev.* **2015**, *44*, 6122–6142.
[43] A. Latorre-Sánchez, J. A. Pomposo, *Polym. Int.* **2016**, *65*, 855–860.
[44] A. M. Hanlon, C. K. Lyon, E. B. Berda, *Macromolecules* **2016**, *49*, 2–14.
[45] O. Altintas, C. Barner-Kowollik, *Macromol. Rapid Commun.* **2016**, *37*, 29–46.
[46] E. Verde-Sesto, A. Arbe, A. J. Moreno, D. Cangialosi, A. Alegría, J. Colmenero, J. A. Pomposo, *Mater. Horiz.* **2020**, *7*, 2292–2313.
[47] H. Frisch, B. T. Tuten, C. Barner-Kowollik, *Isr. J. Chem.* **2020**, *60*, 86–99.
[48] J. Chen, E. S. Garcia, S. C. Zimmerman, *Acc. Chem. Res.* **2020**, *53*, 1244–1256.
[49] Y. Liu, Y. Bai, *ACS Appl. Bio Mater.* **2020**, *3*, 4717–4746.
[50] M. A. M. Alqarni, C. Waldron, G. Yilmaz, C. R. Becer, *Macromol. Rapid Commun.* **2021**, *42*, 2100035.
[51] A. Sathyan, L. Deng, T. Loman, A. R. A. Palmans, *Catal. Today* **2023**, *418*, 114116.
[52] S. Wijker, A. R. A. Palmans, *ChemPlusChem* **2023**, *88*, e202300260.
[53] I. Asenjo-Sanz, T. Claros, E. González, J. Pinacho-Olaciregui, E. Verde-Sesto, J. A. Pomposo, *Mater. Lett.* **2021**, *304*, 130622.
[54] J. Chen, K. Li, S. E. Bonson, S. C. Zimmerman, *J. Am. Chem. Soc.* **2020**, *142*, 13966–13973.
[55] B. T. Tuten, D. Chao, C. K. Lyon, E. B. Berda, *Polym. Chem.* **2012**, *3*, 3068–3071.
[56] L. Oria, R. Aguado, J. A. Pomposo, J. Colmenero, *Adv. Mater.* **2010**, *22*, 3038–3041.
[57] C. S. Mahon, C. J. McGurk, S. M. D. Watson, M. A. Fascione, C. Sakonsinsiri, W. B. Turnbull, D. A. Fulton, *Angew. Chem. Int. Ed.* **2017**, *56*, 12913–12918.
[58] E. H. H. Wong, G. G. Qiao, *Macromolecules* **2015**, *48*, 1371–1379.
[59] O. Galant, H. B. Donmez, C. Barner-Kowollik, C. E. Diesendruck, *Angew. Chem. Int. Ed.* **2021**, *60*, 2042–2046.
[60] H. Rothfuss, N. D. Knöfel, P. Tzvetkova, N. C. Michenfelder, S. Baraban, A.-N. Unterreiner, P. W. Roesky, C. Barner-Kowollik, *Chem. Eur. J.* **2018**, *24*, 17475–17486.

[61] S. Thanneeru, S. S. Duay, L. Jin, Y. Fu, A. M. Angeles-Boza, J. He, *ACS Macro Lett.* **2017**, *6*, 652–656.
[62] Y. Li, J. Wen, M. Qin, Y. Cao, H. Ma, W. Wang, *ACS Biomater. Sci. Eng.* **2017**, *3*, 979–989.
[63] C. A. Tooley, S. Pazicni, E. B. Berda, *Polym. Chem.* **2015**, *6*, 7646–7651.
[64] J. L. Bohlen, B. Kulendran, H. Rothfuss, C. Barner-Kowollik, P. W. Roesky, *Polym. Chem.* **2021**, *12*, 4016–4021.
[65] N. D. Knöfel, H. Rothfuss, J. Willenbacher, C. Barner-Kowollik, P. W. Roesky, *Angew. Chem. Int. Ed.* **2017**, *56*, 4950–4954.
[66] J. Jeong, Y.-J. Lee, B. Kim, B. Kim, K.-S. Jung, H. Paik, *Polym. Chem.* **2015**, *6*, 3392–3397.
[67] M. A. Reith, S. Kardas, C. Mertens, M. Fossépré, M. Surin, J. Steinkoenig, F. E. Du Prez, *Polym. Chem.* **2021**, *12*, 4924–4933.
[68] N. D. Knöfel, H. Rothfuss, P. Tzvetkova, B. Kulendran, C. Barner-Kowollik, P. W. Roesky, *Chem. Sci.* **2020**, *11*, 10331–10336.
[69] A. Sanchez-Sanchez, A. Arbe, J. Kohlbrecher, J. Colmenero, J. A. Pomposo, *Macromol. Rapid Commun.* **2015**, *36*, 1592–1597.
[70] Z. Hu, H. Pu, *Eur. Polym. J.* **2021**, *143*, 110194.
[71] S. Gillhuber, J. O. Holloway, H. Frisch, F. Feist, F. Weigend, C. Barner-Kowollik, P. W. Roesky, *Chem. Commun.* **2023**, *59*, 4672–4675.
[72] W. Wang, J. Wang, S. Li, C. Li, R. Tan, D. Yin, *Green Chem.* **2020**, *22*, 4645–4655.
[73] R. Upadhya, N. S. Murthy, C. L. Hoop, S. Kosuri, V. Nanda, J. Kohn, J. Baum, A. J. Gormley, *Macromolecules* **2019**, *52*, 8295–8304.
[74] J. Engelke, B. T. Tuten, R. Schweins, H. Komber, L. Barner, L. Plüschke, C. Barner-Kowollik, A. Lederer, *Polym. Chem.* **2020**, *11*, 6559–6578.
[75] A. Sanchez-Sanchez, S. Akbari, A. Etxeberria, A. Arbe, U. Gasser, A. J. Moreno, J. Colmenero, J. A. Pomposo, *ACS Macro Lett.* **2013**, *2*, 491–495.
[76] A. Sanchez-Sanchez, S. Akbari, A. J. Moreno, F. L. Verso, A. Arbe, J. Colmenero, J. A. Pomposo, *Macromol. Rapid Commun.* **2013**, *34*, 1681–1686.
[77] J. Rubio-Cervilla, E. González, J. A. Pomposo, *Nanomaterials* **2017**, *7*, 341.
[78] S. Basasoro, M. Gonzalez-Burgos, A. J. Moreno, F. L. Verso, A. Arbe, J. Colmenero, J. A. Pomposo, *Macromol. Rapid Commun.* **2016**, *37*, 1060–1065.
[79] R. A. Patel, S. Colmenares, M. A. Webb, *ACS Polym. Au* **2023**, https://doi.org/10.1021/acspolymersau.3c00007.
[80] Z. Ruan, S. Li, A. Grigoropoulos, H. Amiri, S. L. Hilburg, H. Chen, I. Jayapurna, T. Jiang, Z. Gu, A. Alexander-Katz, C. Bustamante, H. Huang, T. Xu, *Nature* **2023**, *615*, 251–258.
[81] M. Artar, E. R. J. Souren, T. Terashima, E. W. Meijer, A. R. A. Palmans, *ACS Macro Lett.* **2015**, *4*, 1099–1103.
[82] J. Chen, J. Wang, Y. Bai, K. Li, E. S. Garcia, A. L. Ferguson, S. C. Zimmerman, *J. Am. Chem. Soc.* **2018**, *140*, 13695–13702.
[83] B. F. Patenaude, E. B. Berda, S. Pazicni, *Polym. Chem.* **2022**, *13*, 677–683.
[84] R. C. Paul, B. R. Sreenathan, *Indian J. Chem.* **1966**, *4*, 382.
[85] P. H. Maag, F. Feist, H. Frisch, P. W. Roesky, C. Barner-Kowollik, *Macromolecules* **2022**, *55*, 9918–9924.
[86] A. Sathyan, S. Croke, A. M. Pérez-López, B. F. M. de Waal, A. Unciti-Broceta, A. R. A. Palmans, *Mol. Syst. Des. Eng.* **2022**, *7*, 1736–1748.
[87] A. Sathyan, T. Loman, L. Deng, A. R. A. Palmans, *Nanoscale* **2023**, *15*, 12710–12717.
[88] L. Deng, L. Albertazzi, A. R. A. Palmans, *Biomacromolecules* **2022**, *23*, 326–338.
[89] J. Chen, J. Wang, K. Li, Y. Wang, M. Gruebele, A. L. Ferguson, S. C. Zimmerman, *J. Am. Chem. Soc.* **2019**, *141*, 9693–9700.
[90] T. M. Xiong, E. S. Garcia, J. Chen, L. Zhu, A. J. Alzona, S. C. Zimmerman, *Chem. Commun.* **2022**, *58*, 985–988.
[91] E. S. Garcia, T. M. Xiong, A. Lifschitz, S. C. Zimmerman, *Polym. Chem.* **2021**, *12*, 6755–6760.
[92] Y. Zeng, T. Xu, X.-F. Hou, J. Liu, C. Liu, Z. Chang, J. Fang, D. Chen, *ACS Appl. Polym. Mater.* **2023**, https://doi.org/10.1021/acsapm.3c00390.
[93] K. Mundsinger, B. T. Tuten, L. Wang, K. Neubauer, C. Kropf, M. L. O'Mara, C. Barner-Kowollik, *Angew. Chem. Int. Ed.* **2023**, *62*, e202302995.
[94] J. F. Hofmann, A. H. Roos, F.-J. Schmitt, D. Hinderberger, W. H. Binder, *Angew. Chem. Int. Ed.* **2023**, *62*, e202015179.
[95] S. Liu, M. Tang, J. Pang, J. Hu, W. Chen, J. Cheng, Z. Liu, H. Zhao, R. Tan, *ACS Sustainable Chem. Eng.* **2022**, *10*, 11760–11772.
[96] A. E. Izuagbe, V. X. Truong, B. T. Tuten, P. W. Roesky, C. Barner-Kowollik, *Macromolecules* **2022**, *55*, 9242–9248.

Manuscript received: August 11, 2023
Accepted manuscript online: October 18, 2023
Version of record online: ■■, ■■

Minireviews

Catalysis

K. Mundsinger, A. Izuagbe, B. T. Tuten,* P. W. Roesky,* C. Barner-Kowollik* e202311734

Single Chain Nanoparticles in Catalysis

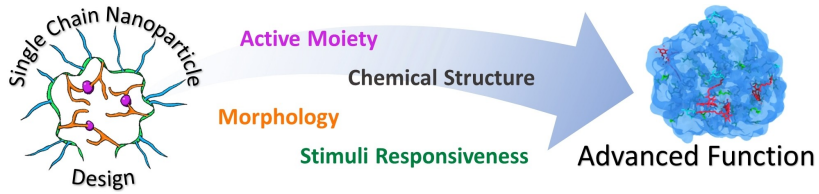

Single chain nanoparticles (SCNPs) are a fascinating macromolecular materials class inspired by natural macromolecules such as enzymes. The current minireview explores their use and potential as versatile catalysts.